

Erosive wear characteristics of multi-fiber reinforced polyester under different operating conditions

This content has been downloaded from IOPscience. Please scroll down to see the full text.

2016 IOP Conf. Ser.: Mater. Sci. Eng. 114 012113

(<http://iopscience.iop.org/1757-899X/114/1/012113>)

View [the table of contents for this issue](#), or go to the [journal homepage](#) for more

Download details:

IP Address: 103.53.34.12

This content was downloaded on 04/03/2016 at 04:12

Please note that [terms and conditions apply](#).

Erosive wear characteristics of multi-fiber reinforced polyester under different operating conditions

U K Debnath¹, M A Chowdhury¹ and D M Nuruzzaman²

¹ Department of Mechanical Engineering, Dhaka University of Engineering and Technology, Gazipur, Bangladesh

² Faculty of Manufacturing Engineering, University Malaysia Pahang, Malaysia

E-mail: dewan052005@yahoo.com

Abstract. Composite materials are used in a wide range of applications. The erosion properties of combination of glass, jute and carbon fiber-reinforced polyester were analyzed in this study. Randomly-shaped silica (SiO₂) particles of various sizes (300–355µm, 355–500µm, and 500–600µm) were selected as the erosive element. Impingement angles between 15–90°, impingement velocities between 30–50 m/sec, and stand-off distances of 15–25 mm at ambient temperature were selected. During experiment, the maximum erosion of the tested composite occurred at 60° impingement angle, indicating a semi-ductile nature of the test material. Erosion increased with impact velocity and decreased with stand-off distance. In a dimensional analysis, erosion efficiency (η) and the relationship between friction and erosion were established. Test results were evaluated using Taguchi's concept to minimize the observations needed, and ANOVA was used to identify interactions between tested parameters and to identify the most significant parameters. The S/N ratio indicates that there is only percentage of deviation between the predicted and experimental results. In further, sophisticated analyses and GMDH methods were employed, and surface damage was examined using scanning electron microscopy (SEM) to examine the nature of the wear behaviour.

1. Introduction

In advanced engineering and industrial field, light weight of composite materials has several applications for minimizing the operating as well as initial investment cost. Composite materials are increasingly used in a wide variety of areas as alternatives to conventional polymers, metals, and alloys. Numerous parameters [1-2] including impingement velocity, impingement angle, type, size and shape of the eroded element, nozzle geometry, stand-off distance, temperature, dry and wet conditions, environment, roughness and hardness of the surface, and fiber orientation are related to erosive damage of the target surface. Repeated impact of materials under different test parameters cause material loss and reduce material life. Damage is accelerated by fiber breakage, crack propagation, micro-cracking, deformation, fractures, and ploughing [3] and researchers are investigating the appropriate test parameters to examine for lower levels of erosion. Composite materials exhibit more erosion compared to pure polymers [3-4]. Most of the previous works focused on fiber orientation in either longitudinal, transverse, or another one-directional arrangement, i.e., fibers embedded in the matrix material at a particular angle. To date, there have been no experimental

² Corresponding author



and theoretical studies on multi-fiber reinforced polyester material. Therefore, the goal of this work was to investigate the erosive damage of multi-fiber reinforced polyester under several test conditions both experimentally and theoretically to better understand the erosion behaviour.

2. Experimental details

2.1 Material properties and set-up

The measured mechanical properties of the multi-fiber reinforced polyester are density 2110 kg/m³, tensile strength 2660 MPa and Poisson's ratio 0.696. Before the erosive wear tests all rectangle shaped specimens were cleaned with acetone. Great care was given to ensure clean surface before and after wear tests. Sand and dust particles were cleaned after erosion test with air blasting and then balanced carefully. A sand blast erosive wear testing device was designed and fabricated to carryout the erosion process, as shown in figure 1. The double disc method was used to estimate the impingement velocity of solid particles.

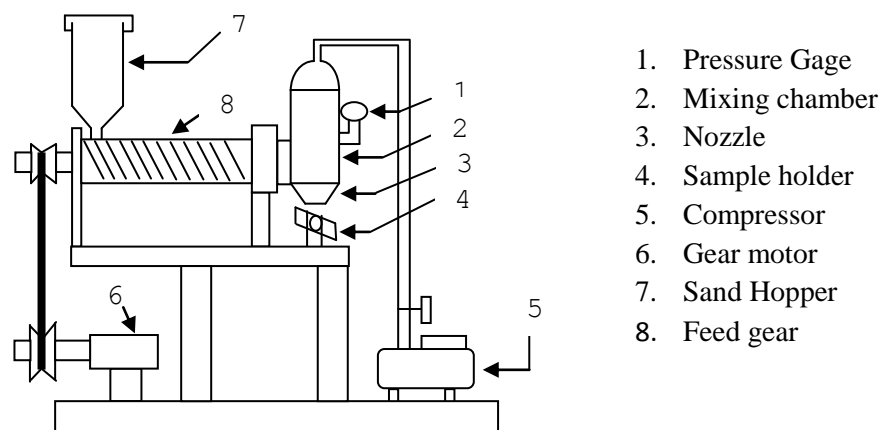


Figure 1. Schematic diagram of the solid particle erosion rig

2.2 Experimental design

Using Taguchi concept, detailed explanation and clarification of controllable experiments to identify the ideal considerations in the DOE (design of experiment) is an effective analysis process. The controlling factors are impact velocity (3 levels: 30(A1), 40 (A2), 50 (A3) m/sec), impingement angle (3 levels: 30(B1), 60(B2), 90(B3) degree), erodent size (3 levels: 300-355(C1), 355-500(C2), 500-600(C3) micron) and standoff distance (3 levels: 15(D1), 20(D2), 25(D3) mm), on the other hand the constant factors are erodent shape (Irregular), erodent feed rate (4.56 gm/sec), test temperature (room temperature), erodent micro-hardness (48-50 HV), nozzle diameter (5mm), Length of nozzle (55mm) and particle density (1036-1043 kg/m³). Considering the L27 (4³) orthogonal array design concept, the significance of four variable factors at four different stages are designated. On the other hand, Taguchi's factorial technique minimizes it to 27 runs, providing a better representation of the results. The number of tests is characterized as a S/N (signal-to-noise) ratio, of which several versions exist based on the type of characteristics. The analyzed ratio related to small amounts of erosive damage is the case of smaller is the better characteristic. Using this approach, this is determined as a logarithmic formulation of the loss function as follows. In the case of less being the improved quality characteristic, this can be estimated using the following formula:

$$\frac{S}{N} = -10 \log \frac{1}{n} (\sum y^2) \quad (1)$$

Where n is the number of observations and y is the observed data. Less is regarded as the improved characteristic with respect to the S/N ratio transformation and is suitable for reducing the erosion rate.

3. Results and discussion

3.1 Influence of impact velocity

During experiments erosion rates showed a sharp, increasing trend, with increases in velocity ranging from 30 to 50 m/sec for the tested composite material (figure 2). Particles created a high impact of kinetic energy at high velocities, resulting in higher impact effect and greater erosion. At 90 degrees impact angle, the kinetic energies of 2071, 2803, 3678, 4625, and 5694 kg-m/sec were estimated for impact velocities of 30, 35, 40, 45, and 50 m/sec, respectively. Kumar et al. [5] and Arjula et al. [6], reported a similar relationship between impingement velocity and erosion rate. The least-squares fitting of actual data was conducted by applying the power law. The relationship between stable erosive wear rate (E) and impingement velocity is stated as a simple power function:

$$E = kv^n \quad (2)$$

Where n the velocity exponent and k the proportionality constant impact on the other parameters. The fitting criteria used are shown in figure 3 using GRAPHWIN software. Using the experimental data, the calculated velocity exponents are in the range of 1.36–1.74 for multi-fiber reinforced polyester at impingement angles between 30 and 90 degrees. The observed velocity exponents are closer to the exponent ranges reported for ductile materials.

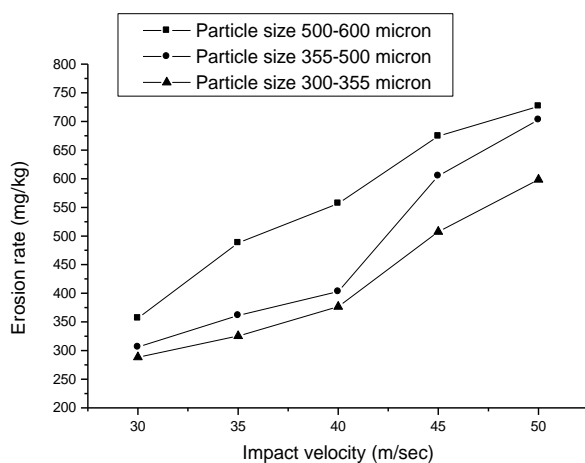


Figure 2. Variation of erosion rate with the variation of impact velocity and erodent size

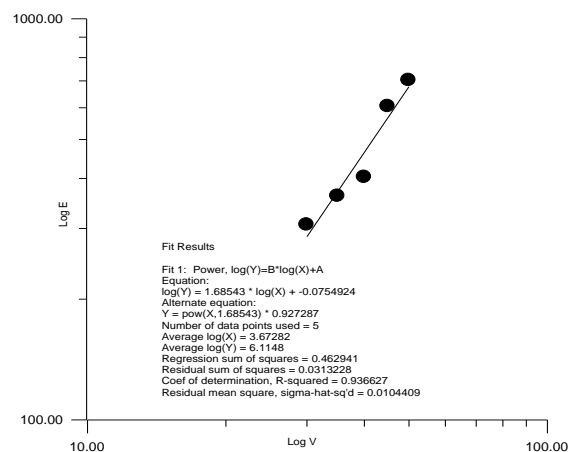


Figure 3. Curve fitting using power law equation for experimental data between erosion rate and impact velocity.

3.2 Influence of impingement angle

The influential characteristics of impact angle on erosion of multi-fiber reinforced polyester at variable particle sizes and impact velocities of 30, 35, 40, 45 and 50 m/sec are shown in figure 4. Erosive damage was highest at 60° impingement for multi-fiber reinforced polyester at several testing conditions. Ductile materials sustain more erosion at level impingement angles (between 15–30°), while brittle surfaces are observed at normal incidence angles (90°). Between 45 and 60° [7], materials with high erosion are deemed semi-ductile. Here, multi-fiber reinforced polyester is regarded as semi-ductile. In general, at low impact angles, erosion was low and the erosion was increased for the impingement angle up to 60° and finally reduced drastically for angle up to 90° as shown in figure 4. Micro-cutting, micro-ploughing, and other damage accumulation processes are the causes of greater erosion in ductile polymers and composites between 15 and 30° due to the enhanced sensitivity of abrasive silica at these angles. For brittle materials, plastic deformation and micro-cracking on the eroded surfaces cause the damage. Several combinations have been noted in previous research of nominally brittle or ductile surfaces. A.P. Harsha et al. [8] reported that surfaces experience ductile, brittle, or semi-ductile conditions when factors such as impingement angle, impact velocity, particle

flux, and erodent properties such as shape, hardness or size are adjusted. In reality, surfaces suffering high levels of erosive damage indicate ductile consequences at smaller angles, and in such cases cutting wear or mechanism is the major concern. Ductile properties are usually signified by the generation of deformation wear, and in such situations less erosion is experienced at higher impact angles. The reverse is true for brittle materials. In our experiments, the semi-ductile nature of multi-fiber reinforced polyester test samples clarifies the micro-cutting, micro-cracking, and visibility of broken fibers is an indication of the combined nature of both ductile and brittle characteristics. Elliptical shape propagation at 45° and 60° impact angles can be explained by the higher divergence of particle flow at lower impact angles.

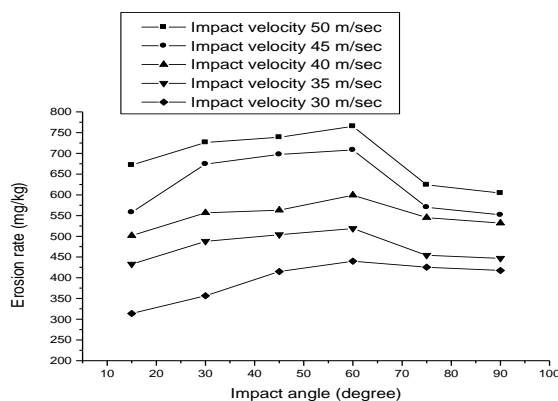


Figure 4. Variation of erosion rate with the variation of impingement angle

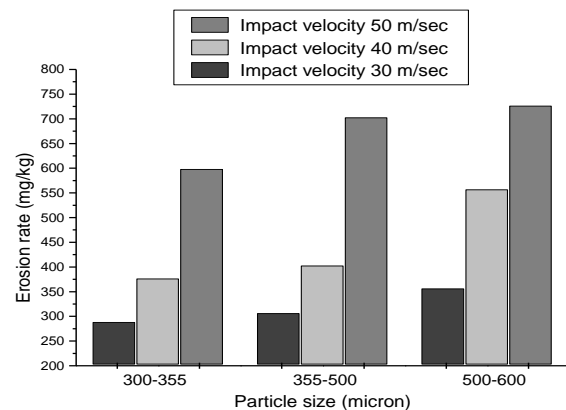


Figure 5. Bar chart showing erosion rate with different particle sizes

3.3 Significance of particle size on erosion

Figure 5 shows the erosion rate for different particle sizes and it is apparent that the erosion rate of the tested material tended to increase with erodent size. Previous studies have emphasized the actual and analytical effects of erodent size when considering solid particle erosion of metals, alloys, polymers, and composites. Most results show similar trends of erosive loss with respect to erodent size. Sandeep Kumar et al. [5] performed erosion experiments using a wide range of particle sizes and observed that lower degrees of particle collision efficiency are responsible for reducing erosive wear with lower erodent sizes. They defined collision efficiency n as a ratio of the number of particles striking a unit area of the surface per unit time to the sum of particles incorporated within the volume of suspension swept by that area per unit time. Larger particles experience retardation just before impact due to the over inertial phenomenon. Therefore, their collision efficiency will be close to unity [9].

3.4 Influence of stand-off distance

Experiments were carried out to examine the effect of the distance between the nozzle and target material on the erosion rate at impact angle 30°, impact velocity 30-50 m/sec, and at three particle sizes. These results of the variation in erosion rate with the variation of stand-off distance are shown in figure 6. It can be seen that the reduction in erosive wear is related to increased distance between nozzle and target material. This is due to the influence of kinetic energy and gravitational force of the sand particle reducing with increasing distance. In addition, when the nozzle and target material are relatively close to each other, particles may strike a small area of the test sample with a high concentration of particle flux but, in the case of large distance, particles may strike a large area of test sample with low concentrations of particle flux.

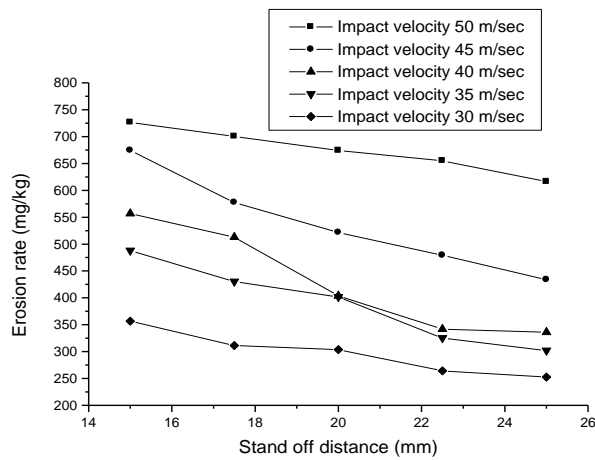


Figure 6. Erosion rate with different stand-off distance at different impact velocity

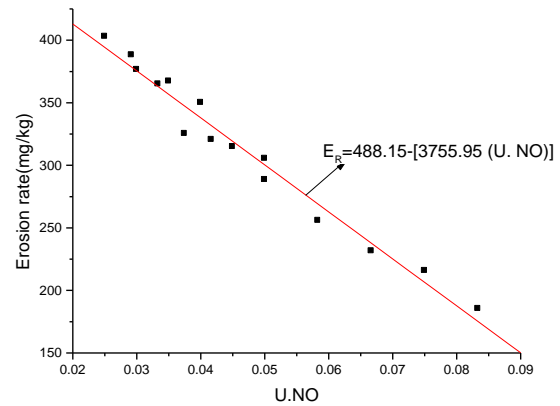


Figure 7. Erosion rate as function of U. No. for multi-fiber reinforced polyester

3.5 Dimensional analysis

Let: $E_R = F(V, f, P, D)$

Where, E_R -Erosion rate= MT^{-1} , V -Impact velocity= LT^{-1} , f - Sand flow rate= MT^{-1} , P -Particle size= L , D -Distance between nozzle and target material= L , So that the dimensional equation is developed as:

$$E_R = K [D/P]^d \quad (3)$$

Where, “d” and “K” are arbitrary constants. The dimensional parameter D/P mentioned in equation (3) is designated as “Uttam Number” and can be expressed in brief as U. No. The relationship between erosion wear (E_R) and U. No. for multi-fiber reinforced polyester material under an impact velocity of 50 m/sec and impact angle 30° is displayed in figure 7. The curve shows that erosion rate decreases linearly with increased U. No. and is represented by the following equation: $E_R = 488.15 - [3755.95 (U. No.)]$ The correlation coefficient (r) was calculated to obtain -0.98 for the test material. Therefore, the actual data figure ensures acceptable recognition with the theoretical model.

3.6 Erosion efficiency

Erosion efficiency (η) can be measured using equation (4):

$$\eta = \frac{2 E_R H V}{V^2 \rho \sin^2 \alpha} \quad (4)$$

Where E_R is the table level of erosive wear, HV is the Vickers hardness of the impacting element (48-50MPa), v is impingement velocity, and ρ is the density of sand (1036-1043kg/m³). The erosion efficiency values of these composites calculated using equation.(4) along with their hardness values and other operating conditions. It is clear that erosion efficiency is not absolutely a material property rather than a material response. There are several alternative operating conditions, such as impingement angle and impact velocity. In the computation methodology, η of the material at normal impact (η normal) changes within 2.11-12.03%, 1.88–13.34%, and 1.34–10.63% for impact velocities 30, 40, and 50 m/s, respectively. The level of η in the case of a specific impact velocity under oblique impact is determined, including multiplying a factor $1/\sin 2\alpha$ with η normal. This relationship between velocity and η has previously been reported by, for example, Arjula and Harsha [10].

3.7 Relation between friction coefficient and erosion rate

The experiments have shown that at the time of contact of high velocity solid particles with the tested materials, the impact velocity is assumed to be generated in parallel and normal components shown in figure 8. Applying force analysis, the friction coefficient can be calculated by:

$$F_x = F \sin \theta \quad \text{and} \quad F = \frac{1}{2} m v^2 \quad \text{or} \quad \mu = \frac{F}{R} \quad \text{or} \quad \mu = \tan \theta$$

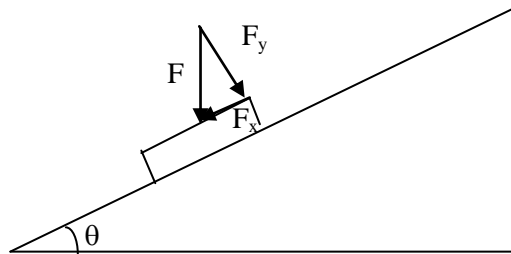


Figure 8. Impact velocity in parallel and normal directions

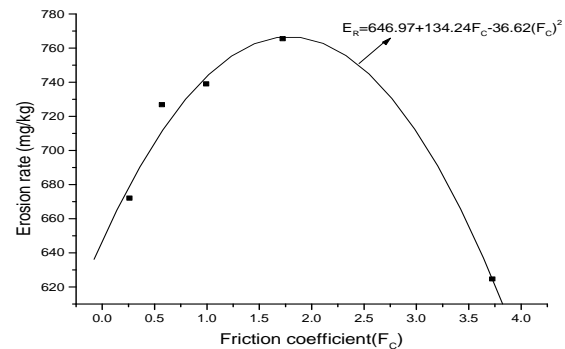


Figure 9. Erosive wear as function of friction coefficient (F_c)

The friction coefficient calculated by the above equation and the corresponding erosion rates at 15-75 degree impact angles and impact velocity 50 m/sec. In figure 9, data show the experimental relationship between erosion rate and the friction coefficient. To justify the experimental relationship in the theoretical context, polynomial regression and correlations were performed using Origin software. Continuous lines indicate regression lines. The correlation coefficients are 0.9756, 0.9092, and 0.97005 for multi-fiber reinforced polyester, respectively, indicating strong positive relationships between erosion rate and friction coefficients for multi-fiber reinforced polyester. The experimental and theoretical data are correlated to an acceptable level.

3.8 Steady state erosion of multi-fiber reinforced polyester

S/N ratio in the context of erosive wear rate indicates the arithmetic mean of two replicates. Considering all the S/N ratios of the erosive wear rates, the average S/N ratio was -51.9867dB. The graphical presentation of the main effect plot of S/N ratio is shown in figure 10(a), MINITAB 17 software was used for this purpose. The relationship between selected control factors are shown in figure 10 (b, c, d), which indicates that to obtain a minimum level of erosion, factors A, B, C, and D are all involved. Comparing the interactions in figure 10(b), the interaction of impact velocity (A) × impingement angle (B) is the most important determinant of erosive wear rate. Even though factors impact velocity (A) and impingement angle (B) have a larger impact on output performance, in the case of combined interrelationships they have a smaller effect on erosive wear rate. In a similar way, while factors impingement angle (B) and particle size (C) separately have a greater effect on output performance, their interaction has a reduced effect on erosive wear rate results.

3.9 ANOVA and the effects of multi-fiber reinforced polyester

Analysis of variance (ANOVA) is a decision-making methodology for confirmation of the significance of the level of effect of the factors considered. A significance level of 5% was considered. The p-values show that the main effects on erosion rate, namely impact velocity, impingement angle, stand-off distance, and erodent size have a high level of significance. In the case of a comparative analysis of interaction between different factors, A*B= interaction with in impact velocity *impingement angle ($p = 0.095$) has a lower p-value than the other two combinations. However, the factor interaction A*C= impact velocity *erodent size ($p = 0.765$), contributes less to erosive wear rate compared to B*C=impingement angle *erodent size ($p=0.997$).

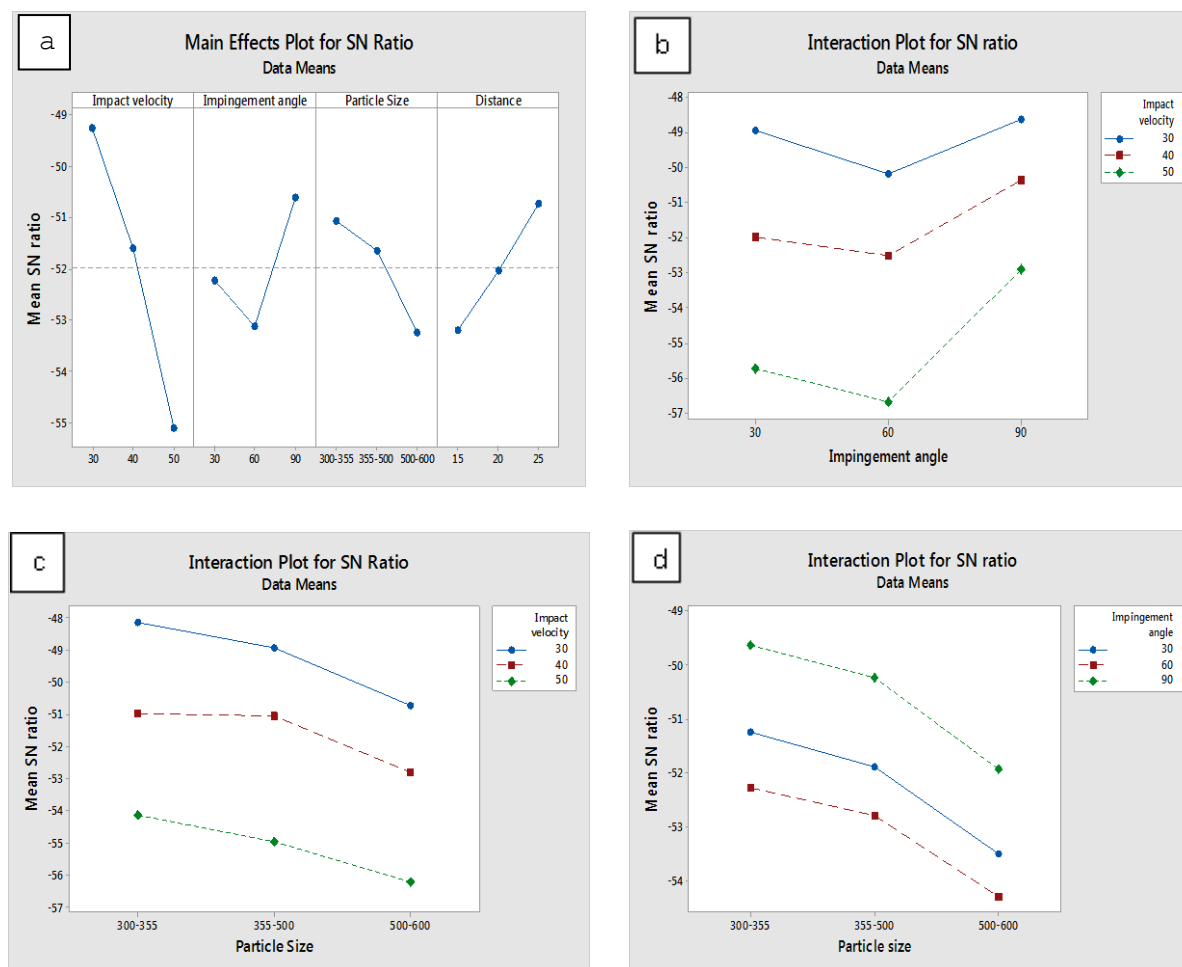


Figure 10. (a) Main effect plot, Interaction graph between (b) Impact velocity× Impingement angle, (c) Particle size× Impact velocity, (d) Particle size× Impingement angle

3.10 Eroding surface morphology of multi-fiber reinforced polyester

The analysis of morphology of multi-fiber reinforced polyester examined by using JEOL JSM 7600F Scanning Electron Microscope (country of origin Japan). SEM micrographs of eroded surfaces of multi-fiber reinforced polyester are shown in figure 11 (a,b). The micrograph 11(a) specifies that multi-fiber reinforced polyester eroded surface at 30° impingement angle is worn by the mechanism of micro-ploughing as well as micro-cutting (marked as 1). The fibers are almost occupied rigidly at location as it is by the ebonite matrix surrounding surface (marked as 1). The fiber matrix non attachment (probably mentioned as de-bonding), brittle fracture characterized matrix and pulverization of fiber are detected in the micrograph (marked as 1). Figure 11(b) illustrates the worn surfaces of multi-fiber reinforced polyester at 60 degree impingement angle. Micro-cracking, micro-cutting and pulverization of matrix and fibers are located as clear evidence in the micrograph (marked as 2) as a consequence of large erosive wear. This is the angle where highest amount of erosion has been noted under all test conditions.

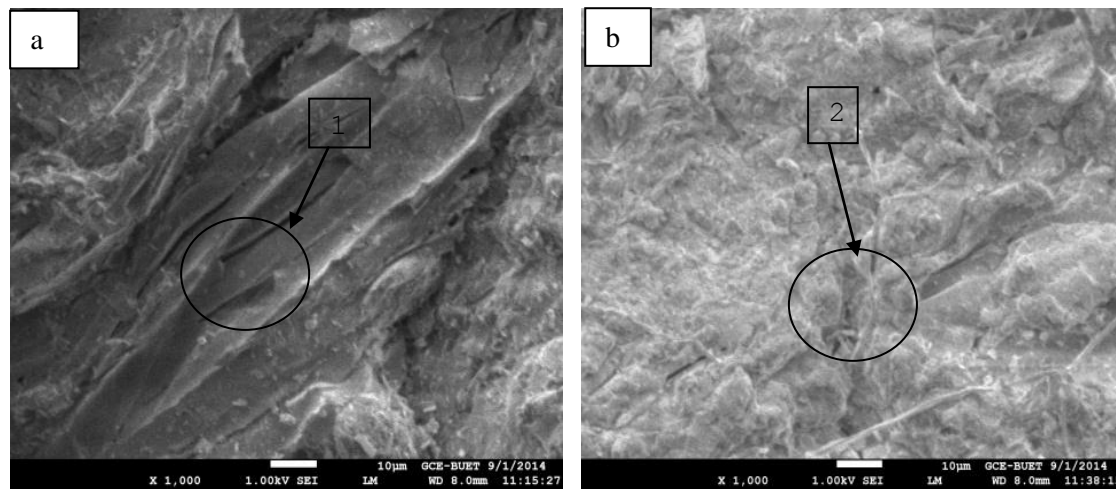


Figure 11. SEM micrograph ($\times 1000$) of eroded multi-fiber reinforced polyester at Impingement angle (a) 30 degree, (b) 60 degree

3.11 Confirmation experiment for multi-fiber reinforced polyester

The measured S/N ratio for wear rates are estimated in connection with the predictive equations:

$$\bar{\eta}_1 = \bar{T} + (\bar{A}_2 - \bar{T}) + (\bar{B}_1 - \bar{T}) + (\bar{C}_3 - \bar{T}) + (\bar{D}_1 - \bar{T}) + [(\bar{A}_2\bar{B}_1 - \bar{T}) - (\bar{A}_2 - \bar{T}) - (\bar{B}_1 - \bar{T})] \quad (5)$$

Where $\bar{\eta}_1$ indicates prediction average value; \bar{T} means overall test results average; \bar{A}_2 , \bar{B}_1 , \bar{C}_3 and \bar{D}_1 is the mean response in relation to factors at designated levels.

Noting combination of like-terms, the equation can be written in reduced form:

$$\bar{\eta}_1 = \bar{A}_2\bar{B}_1 + \bar{C}_3 + \bar{D}_1 - 2\bar{T} \quad (6)$$

A newly combinational factor levels A2, B1, C3 and D1 is considered to predict erosion rate through predicted equation and it is determined as a $\bar{\eta}_1 = -57.947$. The experimental and predicted results are shown in table 1.

Table 1. Results of the confirmation experiments for erosion rate

| Level | Optimal control parameters | |
|---------------------------------|----------------------------|--------------------------|
| | Prediction | Experimental |
| S/N ratio for erosion rate (dB) | A2, B1, C3, D1 -57.94 | A2, B1, C3, D1 -54.59 |

The new generated model is very meaningful for the prediction of erosive wear rate to a justifiable accuracy. The calculated deviation (error level) is 5.79 % is obtained in case of S/N ratio of erosive wear rate.

4. Conclusions

Erosion test results of multi-fiber reinforced polyester have been presented for different operating parameters and the new findings have been reported. The validation of these results and the correlation of erosion with friction, Uttam number, ANOVA, erosion efficiency, S/N ratio, and GMDH is the novel approach for these multi-fiber composites. The morphological analysis provides evidence of the actual wear mechanisms that include micro-cutting, micro-ploughing, micro-cracking and pulverization. At lower impingement angle, erosion is low but increases sharply to reach a maximum level of erosion at 60°, after which it decreases. The confirmation of the material's semi-ductile nature is supported by the highest erosion damage occurring at an angle of 60 degree. The increase in erosion with impact velocity and, probably, kinetic energy level and temperature propagation through the test

area are some unique characteristics of the composite. The power law-based approach ensures that the tested composite group is valid by confirming an exponent value within the range 1.36 to 1.74. The correlation of erosion rate with U. No. and the relationship between erosion rate and friction factor are in good agreement, and can be used as a tool in future studies. The erodent size and stand-off distance provide new insights into the relationship of these parameters with erosion rate. The average S/N ratio of -51.9867 dB and Taguchi design concept ensure the validity of the experimental and theoretical results. The predicted and experimental S/N ratio fluctuations within the range 5.79 % . The use of the ANOVA method explains the contribution of the main factors to erosion individually or as interacting pairs.

5. References

- [1] Arjula S, Harsha AP and Ghosh MK 2008 Solid-particle erosion behavior of high performance thermoplastic polymers *J. Mater. Sci.* **43** 1757–1768
- [2] U.S. Tewari, A.P. Harsha, A.M. Hager and K. Friedrich 2003 Solid particle erosion of carbon fibre- and glass fibre- epoxy composites *Compos. Sci. Technol.* **63** 549–557
- [3] A.P. Harsha, U.S. Tewari and B. Venkataraman 2003 Solid particle erosion behaviour of various polyaryletherketone composites *Wear* **254** 693-712
- [4] N. Miyazaki and T. Hamao 1994 “Solid particle erosion of thermoplastic resins reinforced by short fibers *J. Compos. Mater.* **28** (9) 871-883
- [5] Sandeep Kumar , Bhabani K. Satapathy and Amar Patnaikb 2011 Thermo-mechanical correlations to erosion performance of short carbon fibre reinforced vinyl ester resin composites *Materials and Design* **32** 2260–2268
- [6] Arjula, S , Harsha A.P and Ghosh M.K 2009 Solid Particle Erosion Studies on Polyphenylene Sulfide Composites and Prediction on Erosion Data Using Artificial Neural Networks *Wear* **266** 184-193
- [7] M. Roy, B. Vishwanathan and G. Sundararajan 1994 The solid particle erosion of polymer matrix composites *Wear* **171** 149–161
- [8] A.P. Harsha, Avinash A and Thakre 2007 Investigation on solid particle erosion behavior of polyetherimide and its composites *Wear* **262** 807–818
- [9] H. M Clark and R.b Hartwich 2000 A re-examination of the ‘particle size effect’ in slurry erosion *Wear* **248** 147-161
- [10] Suresh Arjula, A.P. Harsha and M.K. Ghosh 2006 Erosive wear of unidirectional high carbon steel materials *Materials. Letters* **62** 3246–3249